Using the Recovery Phase in Wheelchair Racing to Estimate the Resistance Forces

Vera de Vette

Using the Recovery Phase in Wheelchair Racing to Estimate the Resistance Forces

by

Vera Gabrielle de Vette

in partial fulfilment of the requirements for the degree of

Master of Science in Biomedical Engineering
Track: Neuromusculoskeletal Biomechanics

at the Delft University of Technology,
Faculty of Mechanical, Maritime and Materials Engineering (3mE)

to be defended publicly on Wednesday June 14, 2023 at 10.00 AM

Student number: 5173116

Thesis committee: Prof. dr. H. E. J. Veeger   TU Delft   Chair
                    M. P. van Dijk, MSc.   TU Delft   Supervisor
                    Dr. Ir. A.H.A Stienen   TU Delft   Committee member

Abstract: Insight into in-field mechanical power estimation in wheelchair racing is useful for athletes and coaches. A non-invasive method to estimate mechanical power is by using inertial measurement units (IMUs) to estimate the power lost to resistive forces during wheelchair propulsion. During the recovery phase, no propulsive force acts on the athlete/wheelchair combination and therefore, the deceleration of the athlete/wheelchair combination during this phase is caused by the power lost to resistive forces. The aim of this study was to investigate whether using deceleration in the recovery phase for estimation of resistance using IMUs is applicable in wheelchair racing. To approach the instantaneous velocity of the athlete/wheelchair combination and therefore the deceleration during the recovery phase, the kinematics of the wheelchair and the upper body were measured and used for three different methods. The simplest method is to use the velocity of the wheelchair (v_{wc}), the second method takes the influence of the trunk movement into account ($v_{com,2seg}$) and the last method takes the influence of all upper body segments into account ($v_{com,tot}$). The results of this study indicate that using v_{wc}, $v_{com,2seg}$ or $v_{com,tot}$ for estimating the deceleration during the recovery phase is not yet suitable to provide accurate estimation of the total resistance compared to drag test based results. This indicates that application of this method of estimating resistance forces in the recovery phase is not as straightforward as initially anticipated. Despite the potential benefits of this approach, the results suggest that refinement of this method or development of a new method is necessary to obtain an accurate estimation of the total resistance.

1. Introduction

Mechanical power is a convenient and objective metric to track in wheelchair racing for several reasons. Mechanical power is often used as performance indicator, as the average speed and performance of athletes largely depends on the amount of mechanical power they can sustain over a given distance [1]. Since environmental factors such as wind speed or slope are accounted for when estimating mechanical power, it is an objective measure of the external load of a race or training session [2, 3]. Additionally, monitoring mechanical power can be used for fitness and fatigue assessments [3], which can help prevent overtraining and support training periodisation [4]. This makes estimation of mechanical power a valuable tool for coaches, sport scientists, and athletes.

Power output in wheelchair propulsion can be estimated using the power balance equation [1]. This power balance is based on the free body diagram of the athlete with racing wheelchair system as shown in Figure 1. For wheelchair propulsion this power balance equation can be written as [5]:

$$\begin{aligned} P_{in} &= ma\boldsymbol{v} - P_{out} \\ &= ma\boldsymbol{v} - \left(\boldsymbol{F}_{drag} + \boldsymbol{F}_{roll} + \boldsymbol{F}_{int} + \boldsymbol{F}_{g}\right) \cdot \boldsymbol{v} \end{aligned} \tag{1}$$

where P_{in} is the power generated by the athlete (due to $\boldsymbol{F}_{prop}$), m, $\boldsymbol{a}$ and $\boldsymbol{v}$ are the mass, acceleration vector and velocity vector of the athlete/wheelchair combination, respectively. P_{out} is the power loss due to resistive forces which consist of the air resistance ($\boldsymbol{F}_{air}$), rolling resistance ($\boldsymbol{F}_{roll}$), internal friction ($\boldsymbol{F}_{int}$) and gravitational forces ($\boldsymbol{F}_g$). Put into words, the wheelchair athlete generates power (P_{in}) to (partially) overcome power losses due to resistive forces (P_{out}) resulting in velocity and acceleration of the athlete/wheelchair combination ($ma\boldsymbol{v}$).

In wheelchair sports, there are several measurement systems -such as the SmartWheel or OptiPush- attempting to estimate P_{in} by measuring the force of the hands on the rim and the angular velocity of the wheel [6-9]. However, these systems add a considerable weight to the wheelchair, making them unsuitable for wheelchair racing. Another option is to estimate power output by determining the power lost due to resistive forces (P_{out}) and the velocity and acceleration of the athlete/wheelchair combination ($ma\boldsymbol{v}$).

Depending on the application, there are different options to quantify the resistive forces. For example, rolling resistance is often estimated using drag tests [10]. A drag test is usually performed on a treadmill such that air resistance is
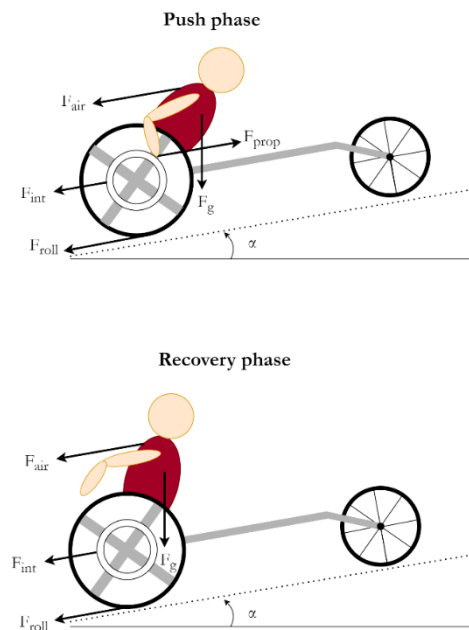

Figure 1. Free body diagram of the athlete with racing wheelchair system in push and recovery phases

2

negligible. The needed force to drag the athlete/wheelchair combination on the treadmill without a slope is attributed to the rolling resistance and internal resistance. For in-field conditions, a coast-down test is often used.

Coast-down tests are based on the second law of Newton. During these tests, the athlete does not apply any force on the hand rim so there is no propulsive force and thus no power generated by the athlete ($P_{in} = 0$). In addition, the athlete does not move, and the system can be considered as a rigid body. Therefore, the wheelchair velocity during coast-down tests is similar to the velocity of the athlete/wheelchair combination. Consequently, the deceleration of the wheelchair during these tests ($ma\boldsymbol{v}$) is due to the power lost due to resistive forces (P_{out}) which is an indication of the total resistance ($\boldsymbol{F}_{roll} + \boldsymbol{F}_{int} + \boldsymbol{F}_{air} + \boldsymbol{F}_{g}$) at a given speed (Eq. (1)) [11-13]. However, changes in the surface, slope or the wheelchair velocity would require an individual coast-down test to accurately estimate mechanical power in different conditions. Therefore, it would be beneficial to obtain an in-field estimation of mechanical power during training or competition such that it requires no extra actions of the athlete.

A non-invasive way of estimating the total resistance is using the recovery phase during wheelchair propulsion. During the recovery phase, the athlete does not apply any force on the hand rim and there is no power generated by the athlete ($P_{in} = 0$). Therefore, comparable to coast down testing, the deceleration of the athlete/wheelchair combination during recovery phase ($ma\boldsymbol{v}$) is an indication of the total ($\boldsymbol{F}_{roll} + \boldsymbol{F}_{int} + \boldsymbol{F}_{air} + \boldsymbol{F}_{g}$) at a given speed. This principle has already been used in wheelchair basketball to estimate the rolling resistance, using the velocity pattern of the wheelchair to estimate the deceleration during recovery phase [14, 15]. However, in contrast to coast-down tests, where the athlete/wheelchair combination behaves as a rigid body, the upper body of the athlete moves during the recovery phase of wheelchair propulsion and thus, the athlete/wheelchair combination does not behave as a rigid body.

During wheelchair propulsion, the upper body segments move with respect to the wheelchair, creating a force of the athlete on the wheelchair ($\boldsymbol{F}_{a/w}$). In the recovery phase, the upper body segments move backwards, creating a $\boldsymbol{F}_{a/w}$ that pushes the wheelchair forwards (see Fig. 2). While during the push phase, the upper body segments of the athlete move forwards with respect to the wheelchair, pushing the wheelchair backwards (see Fig. 2). In other words, by moving the upper body segments a mass redistribution of the athlete/wheelchair combination occurs. Therefore, due to the forces acting on the wheelchair, the wheelchair velocity pattern is not only influenced by the force applied on the hand rim causing an acceleration peak, but also by the mass redistribution due to the arm and trunk swing, causing either an acceleration or deceleration period [16]. Consequently, the velocity of the athlete/wheelchair combination is not equal to the velocity of the wheelchair which makes the estimation of the deceleration of the athlete/wheelchair combination ($ma\boldsymbol{v}$) complicated.

The impact of the mass redistribution on the wheelchair velocity pattern increases with increased speed in wheelchair basketball [16]. However, in wheelchair racing, it is expected that the effect of the mass redistribution in wheelchair racing has less of an impact, since the range of motion of the trunk during wheelchair racing is less than the range of motion of the trunk in wheelchair basketball. For the arm movement, it is worth noting that although the athlete's arms can achieve high velocities at high push frequencies in order to match the high angular velocity of the wheels [17], their mass only accounts for approximately 10% of the total body weight [18]. Consequently, it seems unlikely that the arms have a significant impact on the redistribution of mass. In conclusion, three options are devised to estimate the deceleration of the athlete/wheelchair combination in the recovery phase. The simplest option is to use the velocity pattern of the wheelchair. The second option is to correct the velocity pattern by taking the kinematics of the trunk
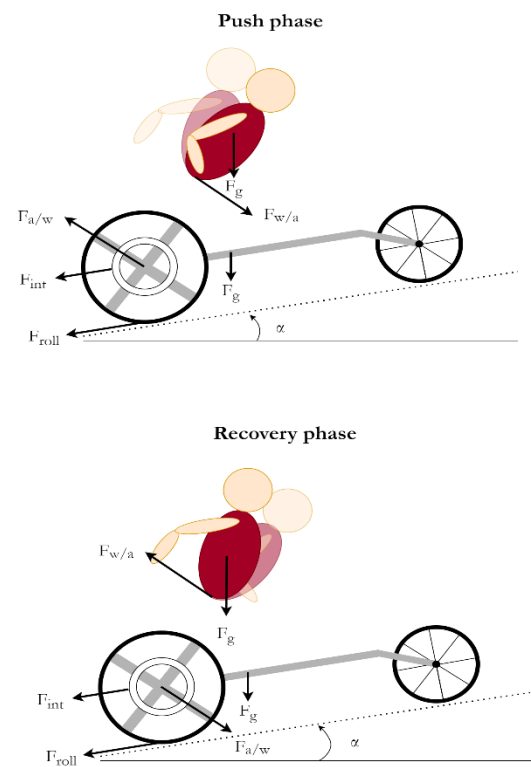

Figure 2. Free body diagram of the athlete with racing wheelchair system in push and recovery phases

into account. The last option is the most thorough but also the most complex by taking the kinematics of all the upper body segments into account.

A promising non-invasive and low-cost method for measuring in-field power output is by using of inertial measurement units (IMUs) [19]. IMUs are small and lightweight sensors that typically consist of an accelerometer, gyroscope, and magnetometer, which measure linear acceleration, angular velocity, and local magnetic field, respectively. Consequently, the velocity of the wheelchair can be obtained by using the output of an IMU on the wheelchair,. Moreover, the output of IMUs can also be used to determine bodily segment kinematics such as orientation and velocity [20]. IMUs also show to be promising in estimation of forces. Changes in rolling resistance due to changed tire pressure or surface can already be measured by IMUs using the deceleration of the wheelchair during coast-down tests [14].

The aim of this study was to investigate whether using the velocity curve of the wheelchair obtained with an IMU during the recovery phase in wheelchair racing is applicable for estimation of the total resistance, independent of trunk and arm motion. Since the inertial forces of the upper body are likely to contribute less to wheelchair velocity variance, it is hypothesised that measuring wheelchair velocity is sufficient for estimation of the deceleration of the athlete/wheelchair combination and thus for estimation of the total resistance. To test this hypothesis, the kinematics of the upper body are also measured to take the effect of the mass redistribution into account and consequently improve the estimation of the deceleration of the athlete/wheelchair combination.

2. Method

2.1. Participants

Two highly skilled racing wheelchair athletes, hereafter referred to as P1 and P2, participated in this study of whom relevant participant data is displayed in Table 1. Prior to the experiment, the participants were informed about the aim and procedure of the study and provided written informed consent to participate in the study. The experiment was approved by the Human Research Ethics Committee (HREC) of Delft University of Technology.

2.2. Procedure

The study aimed to investigate if the recovery phase of racing wheelchair propulsion could be used to estimate the total resistance. Participants used their own racing wheelchairs, which were not identical. The study consisted of three experimental parts. In the first part, participants performed several wheelchair propulsion related movements while force plates measured front and rear wheel forces. An active motion capture system mapped upper body and wheelchair kinematics. The second part involved riding on a large, motorised treadmill at different speeds with a slope of 0.5 degrees or no slope while upper body and wheelchair kinematics were measured using an active motion capture system and two IMUs. For P1, three different speeds were used on the treadmill: 4.86 m/s, 5.55 m/s, and 6.94 m/s. For P2, four different speeds were used on the treadmill: 4.86 m/s, 5.55 m/s, 6.25 m/s, and 6.94 m/s. In the last part, a drag test was performed on the treadmill to measure total resistance. The wheelchair was attached to a load cell with a non-elastic cord parallel to the slope of the treadmill and the athlete with wheelchair was dragged at about 5.55 m/s at a slope of 0.5 degrees.

2.3. Equipment

Various equipment was utilised to collect data during the experiments. Two force plates developed by the VU Amsterdam technical department measured the ground reaction force and its point of application with sample frequency of 200 Hz. A large, motorised treadmill was used to establish a constant speed and slope (Bonte Machinefabriek, Zwolle, The Netherlands). A load cell (S-Type, Revere Transducers, Vishay Precision Group, Toronto, Ontario, Canada) measured the total resistance on the treadmill during the drag test with a sample frequency of 100 Hz. An active motion capture system (Optotrak Certus, NDI, Waterloo, Ontario, Canada) with four camera rigs was used to collect 3D orientation and position data of marker clusters on the head, trunk, upper arm, lower arm, and the wheelchair with a sample frequency of 100 Hz. Additionally, two IMUs (NGIMU, X-IO Technologies, Colorado Springs, CO, United States) collected 3D inertial sensor data of the trunk and wheelchair wheel with a sample frequency of 100 Hz.

2.4. Data pre-processing

2.4.1. Force plate

The ground reaction forces (GRF), and their point of application (POA) were obtained using force plates in a force plate bounded coordinate system. To transform the force plate data into the Optotrak coordinate system, the location and orientation of the force plates were recorded. The POA and GRF data from both force plates were combined to obtain the total ground reaction force and its POA in the Optotrak coordinate system. Any gaps in the raw data were interpolated using spline interpolation if their duration was less than one-sixth of a second.

2.4.2. Drag test

Total resistance (F_{drag}, Eq. (2)) was taken as the mean force measured while athlete/wheelchair combination was dragged at 5.55 m/s. For the gravitational component (F_g) of the total resistance the slope (α) is 0.5 degrees. The rolling resistance (F_{roll}), is the determined as difference between the total resistance and the gravitational component. In Eq. (2) μ_r is the rolling resistance coefficient and F_n is the normal force.

$$
\begin{aligned}
F_{drag} &= F_g + F_{roll} \\
&= m\boldsymbol{g}\sin(\alpha) + \mu_r F_n
\end{aligned}
\tag{2}
$$

2.4.3. IMU

To obtain the velocity of the wheelchair in the riding direction (v_{wc}), the gyroscope data from the wheel IMU were utilised by multiplying the angular velocity around the wheel axis by the wheel radius plus tire thickness. The wheelchair velocity was then used to derive the acceleration of the wheelchair in the riding direction by calculating the derivative of the wheelchair velocity, with a half sample shift being corrected through linear interpolation.

To determine the position of the centre of mass (CoM) of the athlete/wheelchair combination both the wheelchair IMU as well as the trunk IMU were used. This CoM was based on two segments: the lower body and upper body (CoM2seg). To determine the position of the trunk CoM with respect to the wheelchair in the riding direction the gyroscope of the trunk IMU was used. A Madgwick AHRS algorithm was used to estimate the trunk angle from the trunk IMU data [21], which, together with the trunk radius based on the longitudinal distance of the suprasternal notch to the line between both spinae iliaci anterior superior [22], was used to obtain the position of the trunk CoM with respect to the wheelchair. The position of the CoM of the complete athlete/wheelchair combination based on the two segments was derived using the estimated segment weights of the total upper body and lower body. It was assumed that the lower body was fixed with respect to the wheelchair and that the CoM of the lower body moved with the wheelchair. The velocity of the CoM based on two segments in riding direction ($v_{com,2seg}$) was estimated by taking the derivative of the position of the CoM.

2.4.4. Optotrak data

Positions of several bony landmarks were collected and related to the corresponding marker cluster to form 3D segments. Using established conventions, the anatomical coordinate systems [23, 24] and inertial parameters [18, 22, 25] of each segment were calculated. The trajectories of the position and orientation of the segments were using the marker data during wheelchair propulsion. Any gaps in the raw data were interpolated if their duration was less than one-sixth of a second. Using the mass and positions of the upper body segments, a combined CoM of the complete upper body is derived.

To determine a centre of mass of the athlete/wheelchair combination, it was assumed that the lower body was fixed with respect to the wheelchair and that the CoM of the lower body moved with the wheelchair. This CoM of the lower body with wheelchair relative to the

Table 1. Relevant participant data

Subject	Gender	Age	Mass Athlete	Mass Wheelchair	Class
P1	Female	48	60.9 kg	12.1 kg	T54
P2	Male	29	69.3 kg	9.2 kg	T34

wheelchair marker cluster was derived by combining the CoM of the upper body and the POA of the total GRF. This allowed for estimation of a combined CoM of the wheelchair with athlete during the trials. The position of the CoM of the complete athlete/wheelchair combination based on all segments (CoMtot) was derived using the estimated segment weights and positions of the individual upper body segments and the lower body. The velocity of the CoM based on all segments in riding direction ($v_{com,tot}$) was estimated by taking the derivative of the position of the CoM based on all upper body segments.

Similar to the position of the centre of mass based on two segments using IMU data, the position of the CoM using only the upper body and lower body is derived using Optotrak data. To determine with Optotrak data, the mass of all the upper body segments is placed at the CoM of the trunk and a combined upper and lower body CoM is calculated. The velocity of the CoM based on two segments ($v_{com,2seg}$) was estimated by taking the derivative of the position of the CoM based on two segments.

2.4.5. Comparison of Optotrak and IMU data

Given that IMUs can be used in-field, the use of IMU data is preferred over Optotrak data. Therefore, to assess differences between the Optotrak data as reference and the IMU data as test data, the goodness of fit between the IMU data and Optotrak data was assessed using mean squared error.

The mean squared error between Optotrak data and IMU data for wheelchair velocity in riding direction (v_{wc}) indicated a good fit between the two wheelchair velocity curves for both participants (see Appendix A) and therefore, the IMU data-based v_{wc} is be used henceforth. The mean squared error between velocity of the CoM based on the lower and upper body ($v_{com,2seg}$) using Optotrak and IMU data, indicated a relatively good fit between the two CoM velocity curves for both participants. Therefore, $v_{com,2seg}$ using IMU data is used henceforth. Since kinematics of the arms and head were only measured using Optotrak, the CoM velocity based on all upper body segments ($v_{com,tot}$) using Optotrak data is used henceforth.

2.4.6. Coasting sections

During the steady-state parts of the trials, athletes occasionally skip a strike, resulting in a longer recovery phase. If the athlete's trunk remains relatively stationary with respect to the wheelchair during these skipped strikes, the recovery phases are similar to coast-down tests. The deceleration measured during these coasting parts, multiplied by the mass of the athlete/wheelchair combination, should result in a total resistance similar to the measured total resistance during the drag tests (see Eq. (3)).

$$\boldsymbol{F}_g + \boldsymbol{F}_{roll} = m\boldsymbol{a} \tag{3}$$

If present, the missed strikes were manually selected in the wheel's IMU velocity data. The decrease in velocity during these coasting parts in these testing conditions (treadmill) is assumed to be linear since the velocity of the system relative to the world is near zero. In addition, the system mass redistribution effects are considered to be negligible as movement of the trunk relative to the wheelchair is minimal. To determine the mean deceleration during these coasting sections, a first-degree polynomial was fitted to the data.

2.4.7. Recovery phase

As both participants had no high-level spinal cord injury and had adequate trunk function, it was assumed that the recovery phase coincided with backward movement of the trunk. Within every push cycle, detected using a push detection algorithm [26], the interval during which the trunk's angular velocity was positive (i.e., when the trunk was moving backward) was selected as the recovery phase. The deceleration during the recovery phase was determined using the velocity data of three different methods: the wheelchair (WC), the two-segment model centre of mass (CoM2seg) and the total centre of mass (CoMtot). To determine the mean deceleration during the recovery phases, a first-degree polynomial was fitted to the data.

2.5. Data analysis

IMU data and Optotrak data were synchronised using a cross-correlation of the linear velocity of the wheelchair during riding backwards and forwards on a stationary treadmill. Data was assumed to be normally distributed and parametric tests were used (One-way ANOVA and Tukey post hoc test). Curves were shown

using filtered data with a cut off frequency of 6 Hz for visual reasons, however no filtered data were used for data analysis. Mean total resistance with standard deviation and the mean absolute error (MAE) compared to the total resistance obtained with the drag test were reported.

3. Results

3.1. Drag test

The total resistance measured during the drag tests was 9.01 N ± 0.51 and 16.21 N ± 1.33 for P1 and P2, respectively. This is equivalent to a mean acceleration of -0.12 m/s² and -0.21 m/s² during a recovery phase or coast down test for P1 and P2 respectively on a mean slope of 0.5 degrees. The mean gravitational component was 6.25 N and 6.72 N and the mean rolling resistance was 2.76 N and 9.49 N for P1 and P2 respectively (see Fig. 3).

3.2. Coasting sections

Figure 4 shows several manually selected longer coasting sections for both P1 and P2. For P1 all the coasting sections were present in a propulsion section without slope, thus the theoretical acceleration was corrected for the absence of slope. The angular velocity
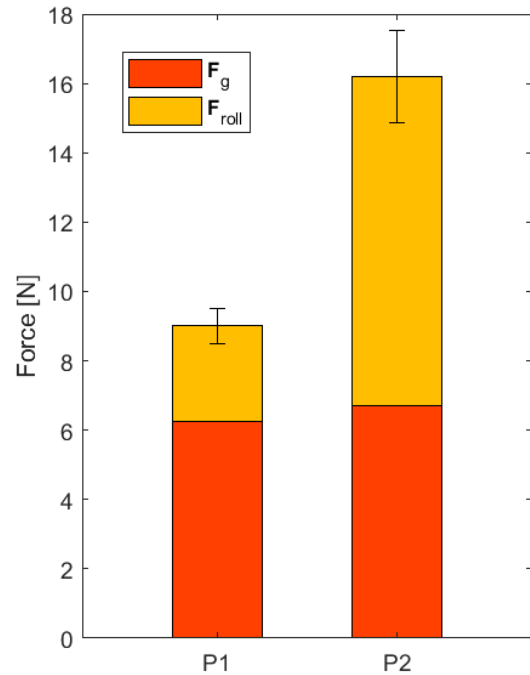

Figure 3. Mean total resistance measured during drag test. Lower part of the bar represents the gravitational component. Upper part of the bar represents the rolling resistance. Error bars display standard deviation.

of the trunk was roughly zero during the coasting sections, such that mass redistribution has little to no effect on the wheelchair velocity. Table 2 displays mean total resistance with standard deviation and MAE for all coasting sections for P1 (only F_{roll}) and for P2 ($F_{roll} + F_g$) using the different methods. For P1, the total resistance is overestimated while for P2 the total resistance in underestimated.

3.3. Recovery phase

Figures 6, 7 and 8 show three seconds of typical velocity patterns of the WC, CoM$_{2seg}$ and CoM$_{tot}$ method respectively for both P1 and P2 for the used treadmill velocities. Mean total resistance and standard deviation determined using the three different methods for all treadmill velocities are shown in Figure 5 for P1 and for P2 ($F_{roll} + F_g$ for both). Appendix B displays all mean total resistance values with standard deviation and MAE. The standard deviation of the determined total resistance increases with increased treadmill velocity, indicating greater variability in the determined total resistance based on the recovery phase. Note that for P1 the

acceleration during the recovery phase is sometimes positive for the CoM$_{tot}$ method at a treadmill velocity of 6.94 m/s, suggesting that the resistance forces are positive (see Figure 5 and 8). Increasing treadmill velocity generally induces higher push frequency except for the treadmill velocity of 6.25 m/s for P2 (see Appendix B). In

Table 2. Mean total resistance based on coasting sections, asterisks (**) denote a significant difference (p<0.001) with theoretical total resistance obtained with drag test. Ratio is the total resistance based on coasting sections divided by the theoretical resistance based on drag test.

Method	P1		P2	
	Total resistance (N)	MAE (N)	Total resistance (N)	MAE (N)
WC	-4.251 ± 1.214 **	1.656	-9.391 ± 2.087 **	6.818
CoM$_{2seg}$	-4.036 ± 1.287 **	1.507	-10.179 ± 1.908 **	6.631
CoM$_{tot}$	-4.183 ± 1.488 **	1.671	-11.813 ± 1.455 **	4.397

addition, the amplitude of the angular velocity of the trunk increases with increasing treadmill velocity (e.g., Fig. 6).

4. Discussion

The aim of this study was to investigate whether using deceleration in the recovery phase for estimation of resistance using IMUs is applicable in wheelchair racing. The results of this study indicate that application of this method of estimating resistance forces in the recovery phase is not as straightforward as initially anticipated and is not yet applicable for in-field estimation of power output. Despite the potential benefits of this approach, the results suggest that refinement of this method or development and application of a different method is necessary to obtain an accurate total resistance estimation.

The main point to address is the accuracy of total resistance measured during the drag tests. The rolling resistance coefficient of P2 in this study is more similar to the coefficient found with coast-down tests on an outdoor track [27], than to that found with a drag test on a treadmill [5], whereas the coefficient of P1 is similar to the one found with a
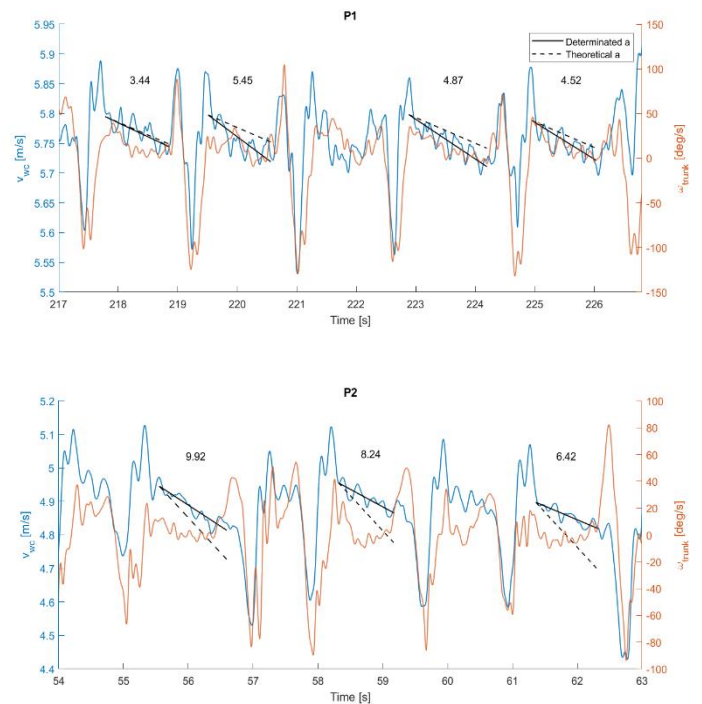

Figure 4. Coasting section during wheelchair propulsion. Wheelchair velocity (blue) and angular velocity of the trunk (orange) are plotted over time. The solid black lines represent the determined deceleration during the coasting sections based on wheelchair velocity. The dashed line represents the theoretical deceleration based on the drag tests. Total resistance estimations are displayed above the coasting sections.

drag test on a treadmill. The rolling resistance determined during long coasting sections due to the missed strikes was about twice as high for P1 compared to the rolling resistance obtained with the drag test (4.25 N vs. 2.76 N). For P2, it was one third of the rolling resistance based on the drag test (2.67 N vs. 9.39 N). However, the rolling resistance for both participants result in rolling resistance coefficients comparable to those found on a treadmill [5]. This raises concerns about the accuracy of the measured force during drag tests. Despite the negligible impact
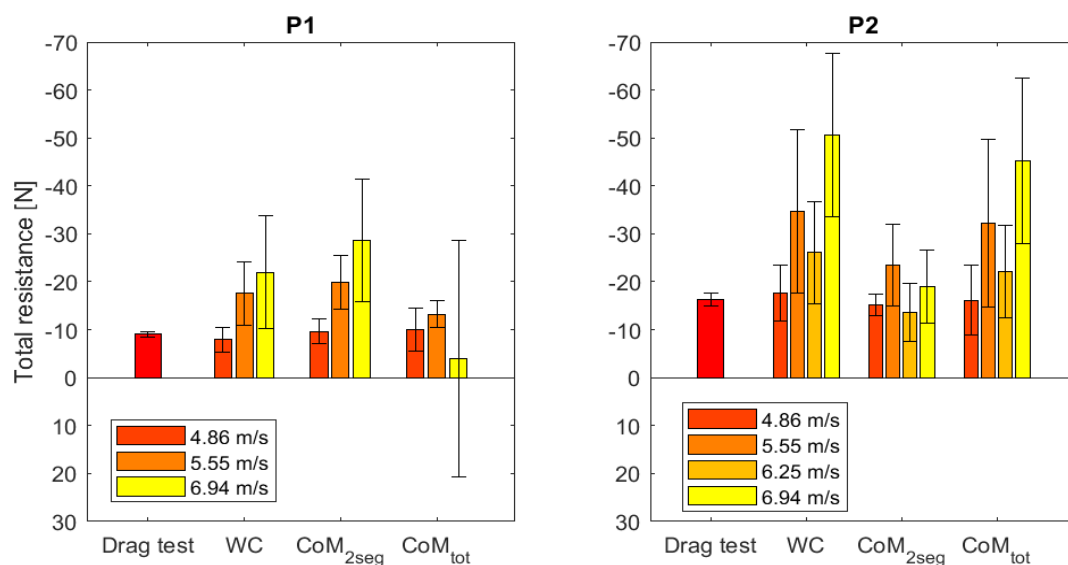

Figure 5. Mean total resistance and standard deviation using different methods and at different treadmill velocities.

of velocity on the velocity-dependent portion of rolling resistance [27], it is recommended for future research to assess the influence of velocity on rolling resistance by conducting drag tests at various speeds. Additionally, conducting drag tests on multiple slopes would improve the accuracy of determining the contributions of rolling resistance and the gravitational component to the total resistance.

The velocity curve of the wheelchair during a push cycle at lower treadmill speeds (see Fig. 6) exhibited three distinct phases similar to previous publications [16]: 1) an acceleration phase, followed by; 2) a period of relatively minor deceleration, or a short coasting section, and finally; 3) a rapid decrease in velocity. At higher velocities, the small coasting section is either significantly reduced or not present at all. However, it is these small coasting sections that theoretically hold the most promise for an accurate estimation of the total resistance. Unfortunately, for the lowest treadmill speed (4.86 m/s) with the longest coasting sections, the mean absolute error is already 2 to 5 N (see Appendix B) which is an error of 20 to 30%. It is interesting to note that the MAE at a treadmill of 6.25 m/s is lower than the MAE at a treadmill velocity of 5.55 m/s for P2. This might be due to the higher variability in push frequency observed at the treadmill velocity of 5.55 m/s resulting in multiple short pushes without short coasting. Overall, these results indicate that the length of the coasting section is a key factor in estimation of total resistance based on the wheelchair velocity. As a result, it is challenging to accurately
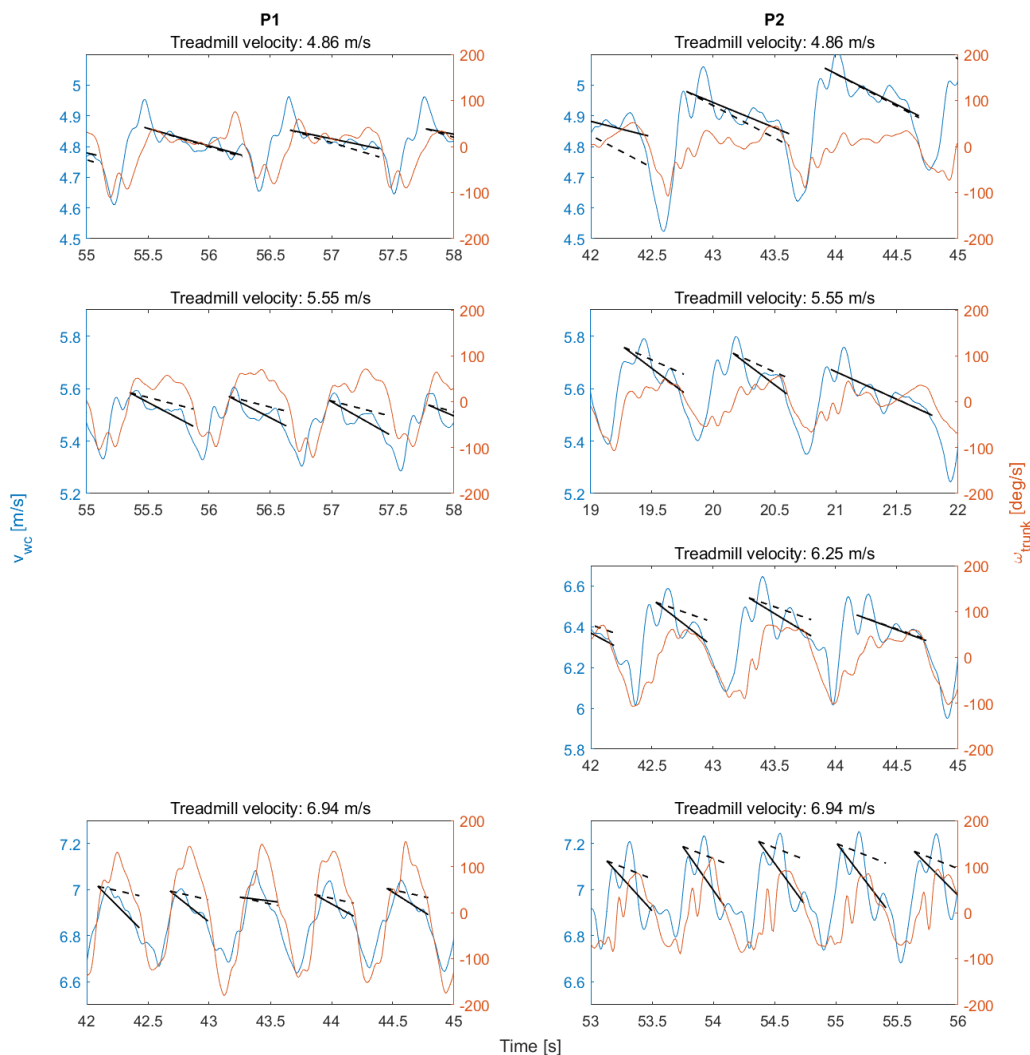

Figure 6. Recovery phases during wheelchair propulsion. Wheelchair velocity (blue) and angular velocity of the trunk (orange) are plotted over time. The solid black lines represent the determined deceleration during the coasting sections based on wheelchair velocity. The dashed line represents the theoretical deceleration based on the drag tests.

estimate rolling resistance in higher propulsion velocities using the methods that rely on the shape of the wheelchair velocity curve.

To improve the estimation of the deceleration of the athlete/wheelchair combination, the influence of the trunk movement was taken into account. In contrast to what was expected, mass redistribution seems to have an influence on the wheelchair velocity, especially in the end of the push cycle. When considering the mass redistribution by correcting for trunk movement, a decrease in the amplitude of the velocity drop is seen (see Fig. 6 and 7). However, this correction does not lead to an improvement of the estimation of the total resistance. Surprisingly, the mean absolute error of the total resistance using the CoM_{2seg} method is found to be higher than that of the WC method. If both the trunk and arm movement are taken into account by using the CoM_{tot} method, the amplitude of the velocity drop is even further reduced (see Fig. 8). It should be noted, however, that the Optotrak data used for the CoM_{tot} method contained significant amount of noise, likely due to a faulty camera rig calibration. However, by using a first-degree polynomial, the impact of these errors is reduced. For the CoM_{tot} method, the mean absolute error of the total resistance is found to be lower than that of the WC method, indicating an improvement of the total resistance estimation as expected. These results indicate that the rapid decrease in wheelchair velocity at the end of the push cycle is (partially) caused by the mass redistribution due to the moving upper body segments.
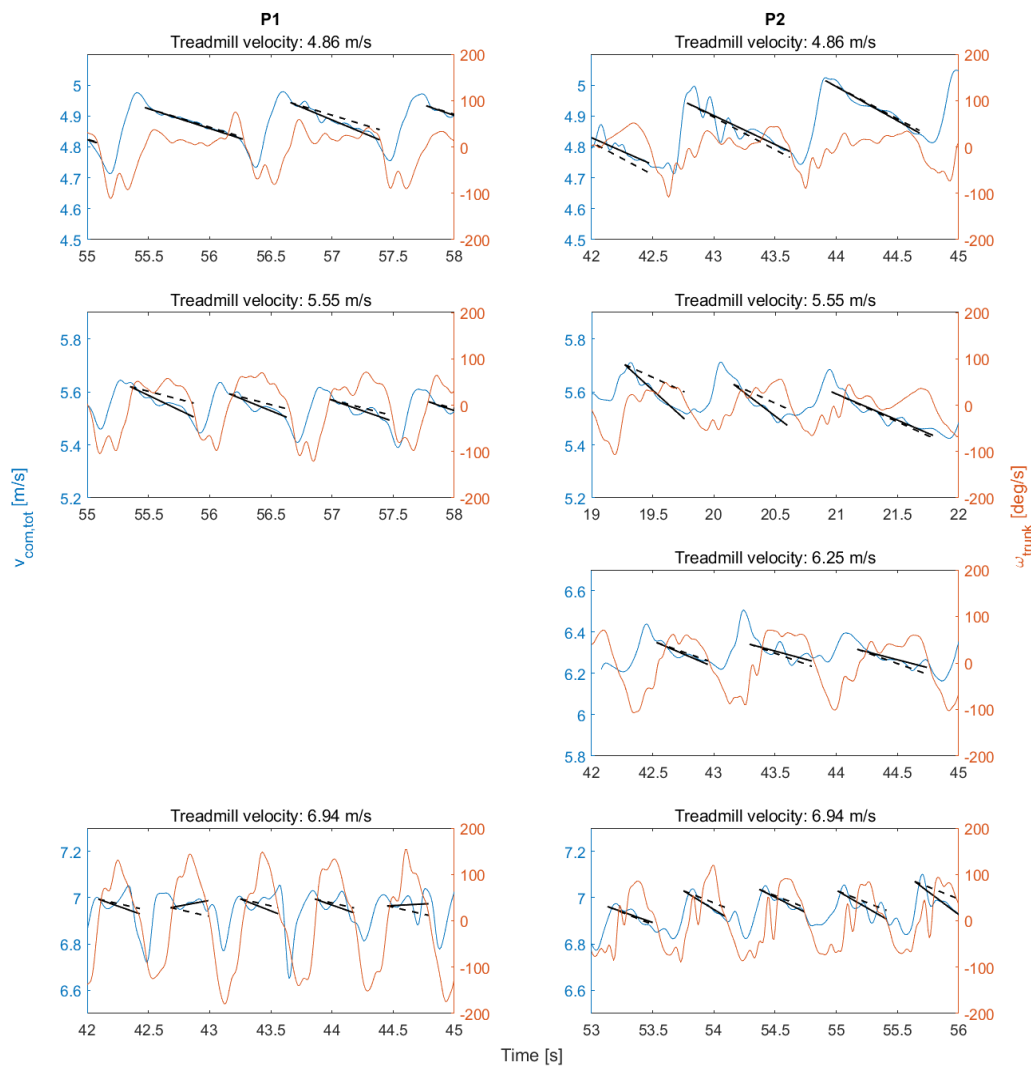

Figure 7. Recovery phases during wheelchair propulsion. Centre of Mass velocity (blue) and angular velocity of the trunk (orange) are plotted over time. The solid black lines represent the determined deceleration during the coasting sections based on wheelchair velocity. The dashed line represents the theoretical deceleration based on the drag tests.

Furthermore, at higher mean propulsion velocities, the influence of the arms on the Centre of Mass velocity becomes more pronounced, likely due to the higher velocities of the arms at these propulsion velocities. However, it is noteworthy that even after correcting for trunk and arm movement, the rapid decrease in velocity did not completely disappear for P1. In contrast, for P2, the amplitude of the velocity drop decreased when using the CoM_tot method. This difference could be attributed to the fact that wheelchair athletes have a non-standard body mass distribution [28], where a standard distribution was assumed in this study. However, by increasing the mass of the upper body with 50%, and thereby overestimating the upper body mass, the remaining dip does not completely vanish (Appendix C). Consequently, it can be refuted that the remaining dip is only caused by an underestimation of the upper body mass. This suggests that, in addition to the mass redistribution, other factors such as technique play a role during the recovery phase.

Another factor that could contribute to these unexpected outcomes is that the current total resistance may be too small (~12 N) to accurately estimate using the recovery phase. As air resistance plays a considerable role in in-field wheelchair racing, the resistances encountered in-field may be higher, making the effect of small deviations in velocity on resistance estimation less significant. In addition, this study was based on a linear decrease in velocity during the recovery phase, such that a first-degree polynomial could be used. This was possible since this study was treadmill based and air resistance is negligible. However, for in-field conditions,
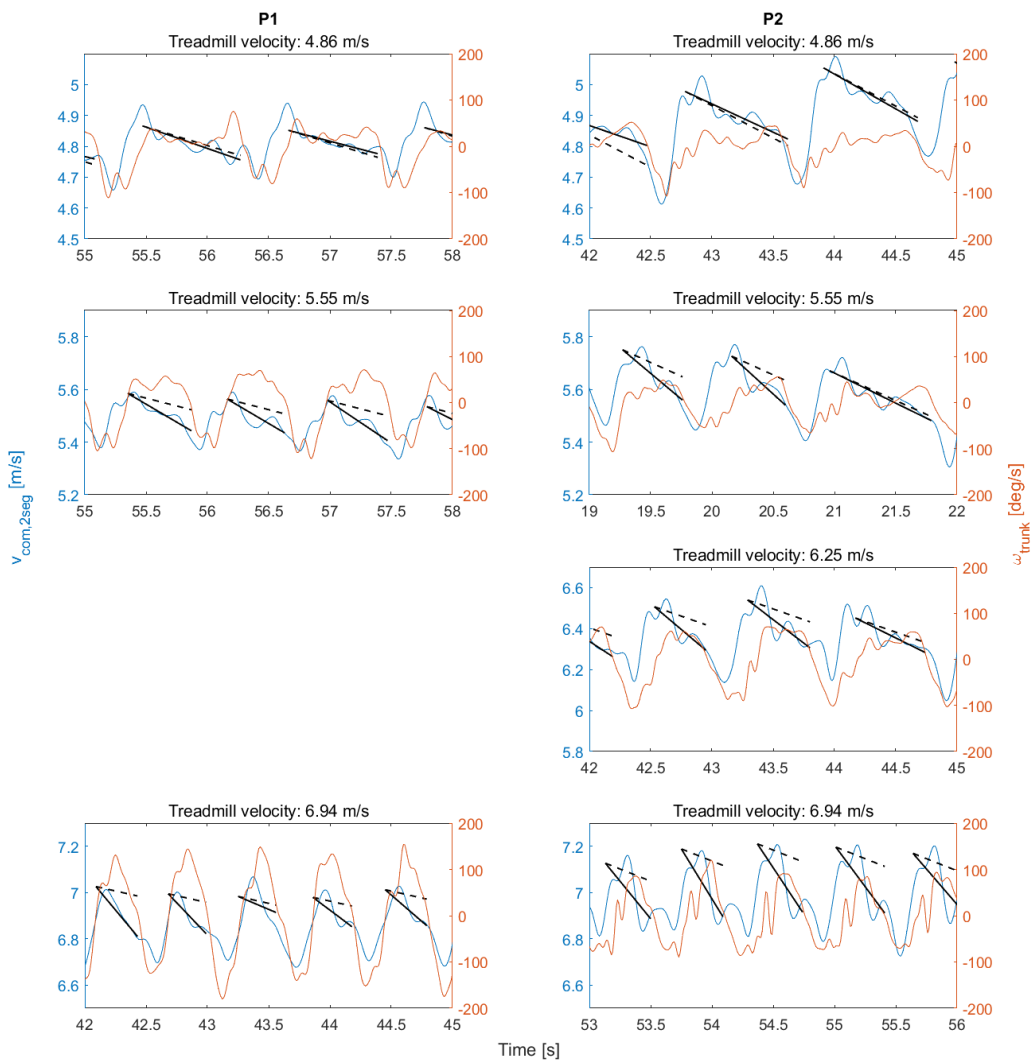

Figure 8. Recovery phases during wheelchair propulsion. Segment-based Centre of Mass velocity (blue) and angular velocity of the trunk (orange) are plotted over time. The solid black lines represent the determined deceleration during the coasting sections based on wheelchair velocity. The dashed line represents the theoretical deceleration based on the drag tests.

air resistance contributes to the total resistance, and since air resistance depends on the squared velocity, a first-degree polynomial could be insufficient to use in-field.

Lastly, it should be noted that the time interval of the recovery phase is estimated based on the sign of the trunk angular velocity. While for athletes with adequate trunk function, this assumption might be reasonable, it may not be accurate for athletes without adequate trunk function. In addition, since wheelchair racing is a technical sport, trunk movement can differ between athletes. Therefore, future research should focus on improving the estimation of the time interval of the recovery phase and therefore the deceleration during the recovery phase, for example by testing how the recovery phase is related to angular trunk velocity for different wheelchair velocities.

If future research confirms the unsuitability of using the recovery phase for power estimation in-field, an alternative practical implication could be the development of a power meter that guides athletes in the timing and duration of performing regular coast-down tests to determine the total resistance. This power meter could initially estimate the total resistance for a given environment, but also allows for recalibration during a training using imposed or self-induced coasting sections. These measurements could then be used to estimate the power across different conditions. Although this option is considered less preferable since it slightly interferes with the behaviour of the athlete, it could serve as a feasible alternative solution.

In conclusion, the findings of this study highlight the complex nature of the factors that influence performance in wheelchair racing. Despite providing valuable insights into the impact of wheelchair athletes' behaviour on deceleration during recovery phases, the results of this study indicate that using the velocity pattern of the wheelchair or the velocity pattern centre of mass of the athlete/wheelchair combination for estimating the deceleration during the recovery phase is not yet accurate. For longer coasting sections the results tend to align more with the expected total resistance. In contrast, the results for higher mean propulsion speeds and consequently shorter recovery phases, show large deviations from the expected total resistance, potentially due to the higher influence of mass redistribution at these velocities. By addressing these factors, researchers can gain a better understanding of the factors that can contribute in wheelchair racing and improve future mechanical power estimations.

References

1. Ingen Schenau, G.J.v. and P.R. Cavanagh, *Power equations in endurance sports.* Journal of Biomechanics, 1990. **23**(9): p. 865-881.
2. Halson, S.L., *Monitoring Training Load to Understand Fatigue in Athletes.* Sports Medicine, 2014. **44**(2): p. 139-147.
3. Mujika, I., *Quantification of Training and Competition Loads in Endurance Sports: Methods and Applications.* International Journal of Sports Physiology and Performance, 2017. **12**(s2): p. S2-9-S2-17.
4. Soligard, T., et al., *How much is too much? (Part 1) International Olympic Committee consensus statement on load in sport and risk of injury.* British Journal of Sports Medicine, 2016. **50**(17): p. 1030.
5. Woude, L.H.V.V.D., et al., *Wheelchair ergonomics and physiological testing of prototypes.* Ergonomics, 1986. **29**(12): p. 1561-1573.
6. de Klerk, R., et al., *Determining and Controlling External Power Output During Regular Handrim Wheelchair Propulsion.* JoVE, 2020(156): p. e60492.
7. van der Scheer, J.W., et al., *Can a 15m-overground wheelchair sprint be used to assess wheelchair-specific anaerobic work capacity?* Medical Engineering & Physics, 2014. **36**(4): p. 432-438.
8. de Groot, S., R.J.K. Vegter, and L.H.V. van der Woude, *Effect of wheelchair mass, tire type and tire pressure on physical strain and wheelchair propulsion technique.* Medical Engineering & Physics, 2013. **35**(10): p. 1476-1482.
9. Mason, B.S., et al., *Effects of Wheel and Hand-Rim Size on Submaximal Propulsion in Wheelchair Athletes.* Medicine & Science in Sports & Exercise, 2012. **44**(1).
10. Ott, J. and J. Pearlman, *Scoping review of the rolling resistance testing methods and factors that impact manual wheelchairs.* J Rehabil Assist Technol Eng, 2021. **8**: p. 2055668320980300.
11. Sauret, C., et al., *Assessment of field rolling resistance of manual wheelchairs.* Journal of rehabilitation research and development, 2012. **49**: p. 63-74.
12. Bascou, J., et al., *A method for the field assessment of rolling resistance properties of manual wheelchairs.* Computer methods in biomechanics and biomedical engineering, 2012. **16**.
13. Hoffman, M.D., et al., *Assessment of Wheelchair Drag Resistance Using a Coasting Deceleration Technique.* American Journal of Physical Medicine & Rehabilitation, 2003. **82**(11).
14. Rietveld, T., et al., *Inertial measurement units to estimate drag forces and power output during standardised wheelchair tennis coast-down and sprint tests.* Sports Biomechanics, 2021: p. 1-19.
15. van Nee, M.M., *Power estimation in wheelchair basketball*, in *Applied Mathematics.* 2017, Delft University of Technology: Delft. p. 119.
16. Vanlandewijck, Y.C., A.J. Spaepen, and R.J. Lysens, *Wheelchair propulsion efficiency: movement pattern adaptations to speed changes.* Medicine & Science in Sports & Exercise, 1994. **26**(11).
17. Wang, Y.T., et al., *Three-Dimensional Kinematics of Wheelchair Propulsion across Racing Speeds.* Adapted Physical Activity Quarterly, 1995. **12**(1): p. 78-89.
18. Plagenhoef, S., F.G. Evans, and T. Abdelnour, *Anatomical Data for Analyzing Human Motion.* Research Quarterly for Exercise and Sport, 1983. **54**(2): p. 169-178.
19. de Vette, V.G., D. Veeger, and M.P. van Dijk *Using Wearable Sensors to Estimate Mechanical Power Output in Cyclical Sports Other than Cycling—A Review.* Sensors, 2023. **23**, DOI: 10.3390/s23010050.
20. Camomilla, V., et al. *Trends Supporting the In-Field Use of Wearable Inertial Sensors for Sport Performance Evaluation: A Systematic Review.* Sensors, 2018. **18**, DOI: 10.3390/s18030873.
21. Madgwick, S.O.H., A.J.L. Harrison, and R. Vaidyanathan. *Estimation of IMU and MARG orientation using a gradient descent algorithm.* in *2011 IEEE International Conference on Rehabilitation Robotics.* 2011.
22. Zatsiorsky, V., *Kinetics of Human Motion.* 2002.
23. Wu, G., et al., *ISB recommendation on definitions of joint coordinate system of various joints for the reporting of human joint motion—part I: ankle, hip, and spine.* Journal of Biomechanics, 2002. **35**(4): p. 543-548.
24. Wu, G., et al., *ISB recommendation on definitions of joint coordinate systems of various joints for the reporting of human joint motion—Part II: shoulder, elbow, wrist and hand.* Journal of Biomechanics, 2005. **38**(5): p. 981-992.
25. de Leva, P., *Adjustments to Zatsiorsky-Seluyanov's segment inertia parameters.* Journal of Biomechanics, 1996. **29**(9): p. 1223-1230.
26. van der Slikke, R., et al., *Push Characteristics in Wheelchair Court Sport Sprinting.* Procedia Engineering, 2016. **147**: p. 730-734.
27. Fuss, F., *Influence of mass on the speed of wheelchair racing.* Sports Engineering, 2009. **12**: p. 41-53.
28. Lewis, A.R., et al., *The Effects of Personalized Versus Generic Scaling of Body Segment Masses on Joint Torques During Stationary Wheelchair Racing.* J Biomech Eng, 2019. **141**(10).

Appendix A

Table A1. Goodness of fit between IMU data and Optotrak data

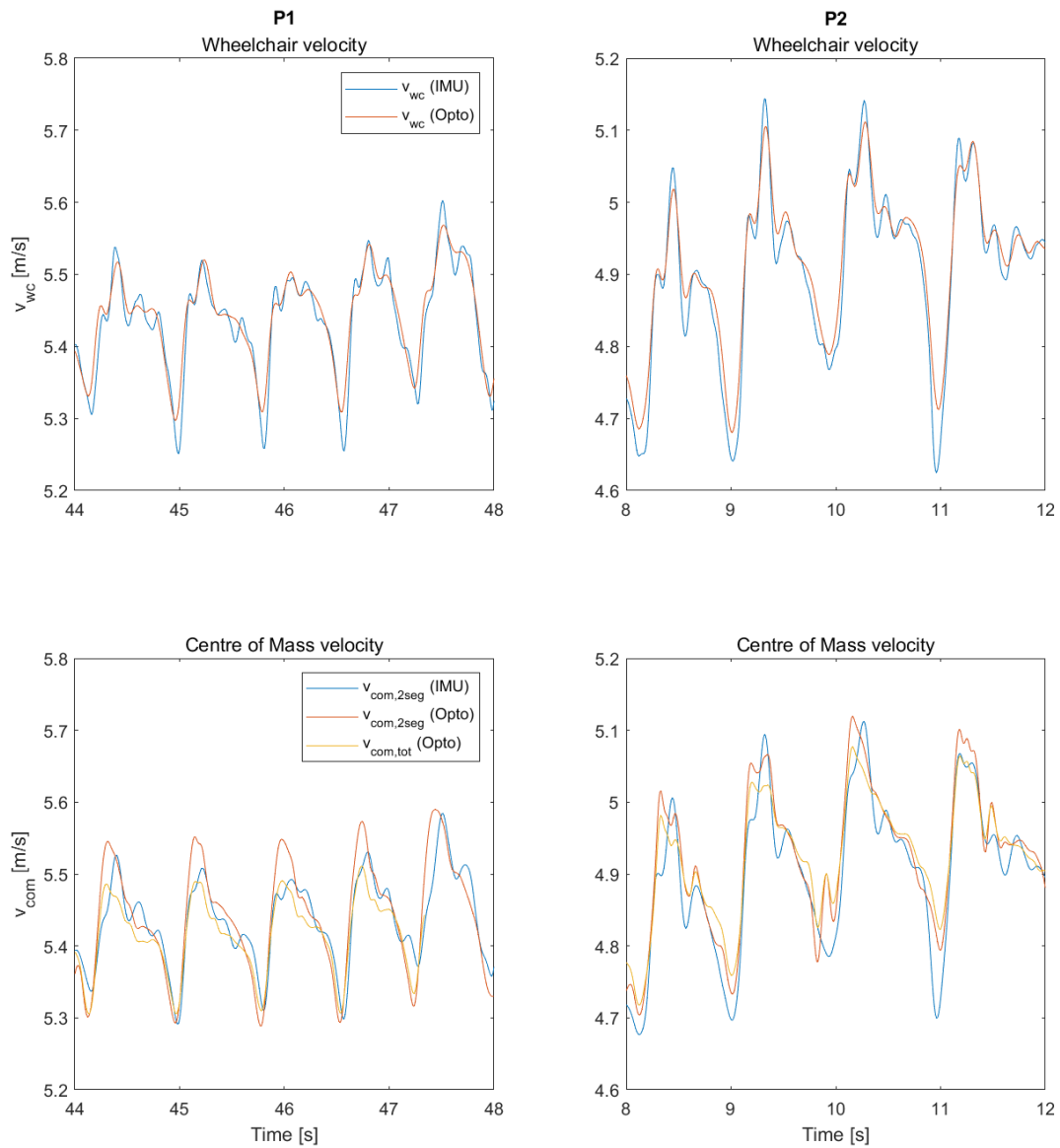| Method	Mean squared error (m/s)^2	
	P1	**P2**
WC	0.0063	0.0053
CoM$_{2seg}$	0.0911	0.0242

Figure A1. Typical velocity pattern using different methods and measurements systems (IMUs and Optotrak).

Appendix B

Table B1. Mean total resistance with standard deviation based on the recovery phases. Asterisks denote significant difference with the total resistance based on the drag test (* = p<0.05, ** = p<0.01. Ratio is the total resistance based on the recovery phases divided by the total resistance based on the drag test.

| Method	Treadmill velocity (m/s)	P1			P2		
		Total resistance [N]	MAE [N]	Push frequency [Hz]	Total resistance [N]	MAE [N]	Push frequency [Hz]
WC	4.86	-7.935 ± 2.567 **	2.109	0.85	-16.152 ± 7.285 *	5.363	0.83
	5.55	-17.529 ± 6.550 **	9.474	1.23	-32.246 ± 17.454 **	17.245	1.07
	6.25				-22.115 ± 9.601 **	7.639	1.00
	6.94	-22.010 ± 11.681 **	14.270	1.53	-45.226 ± 17.352 **	29.288	1.41
CoM$_{2seg}$	4.86	-9.654 ± 2.566 **	2.162	0.85	-17.728 ± 5.847	4.263	0.83
	5.55	-19.965 ± 5.603 **	11.457	1.23	-34.717 ± 17.040 **	19.184	1.07
	6.25				-26.107 ± 10.644 **	10.394	1.00
	6.94	-28.665 ± 12.841 **	19.999	1.53	-50.548 ± 17.009 **	34.340	1.41
CoM$_{tot}$	4.86	-10.069 ± 4.490 **	3.438	0.85	-15.202 ± 2.179 **	2.001	0.83
	5.55	-13.236 ± 2.728 **	4.283	1.23	-23.545 ± 8.518 **	8.867	1.07
	6.25				-13.652 ± 6.103 **	4.806	1.00
	6.94	-3.949 ± 24.709 **	18.445	1.53	-19.039 ± 7.5789 **	5.943	1.41

Appendix C
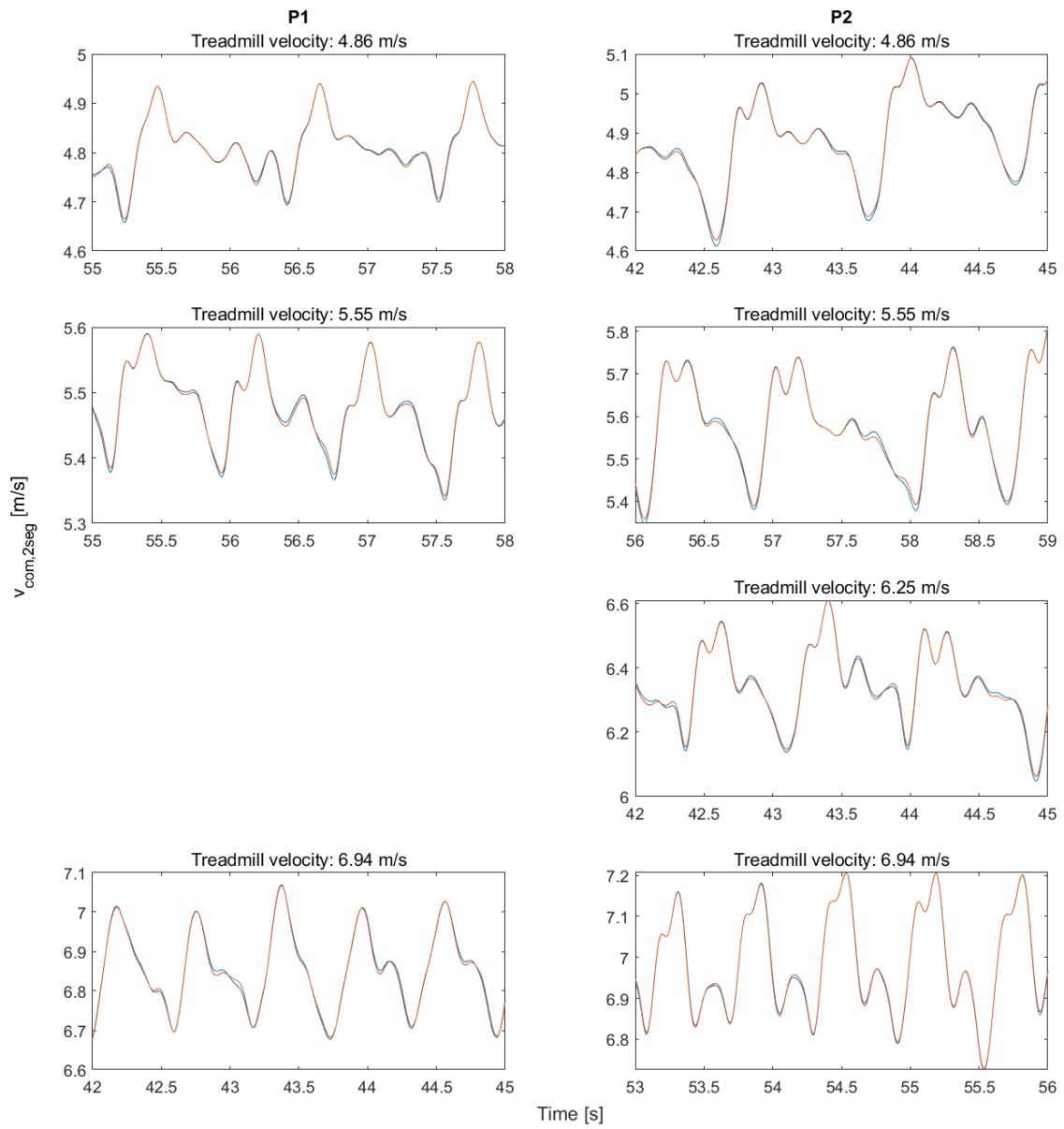
Figure C1. Velocity of the Centre of Mass using the two-segment model plotted over time. The blue line represents the $v_{com,2seg}$ estimation using standard body mass distribution. The orange line represent the $v_{com,2seg}$ estimation using increased upper body mass of 50%.
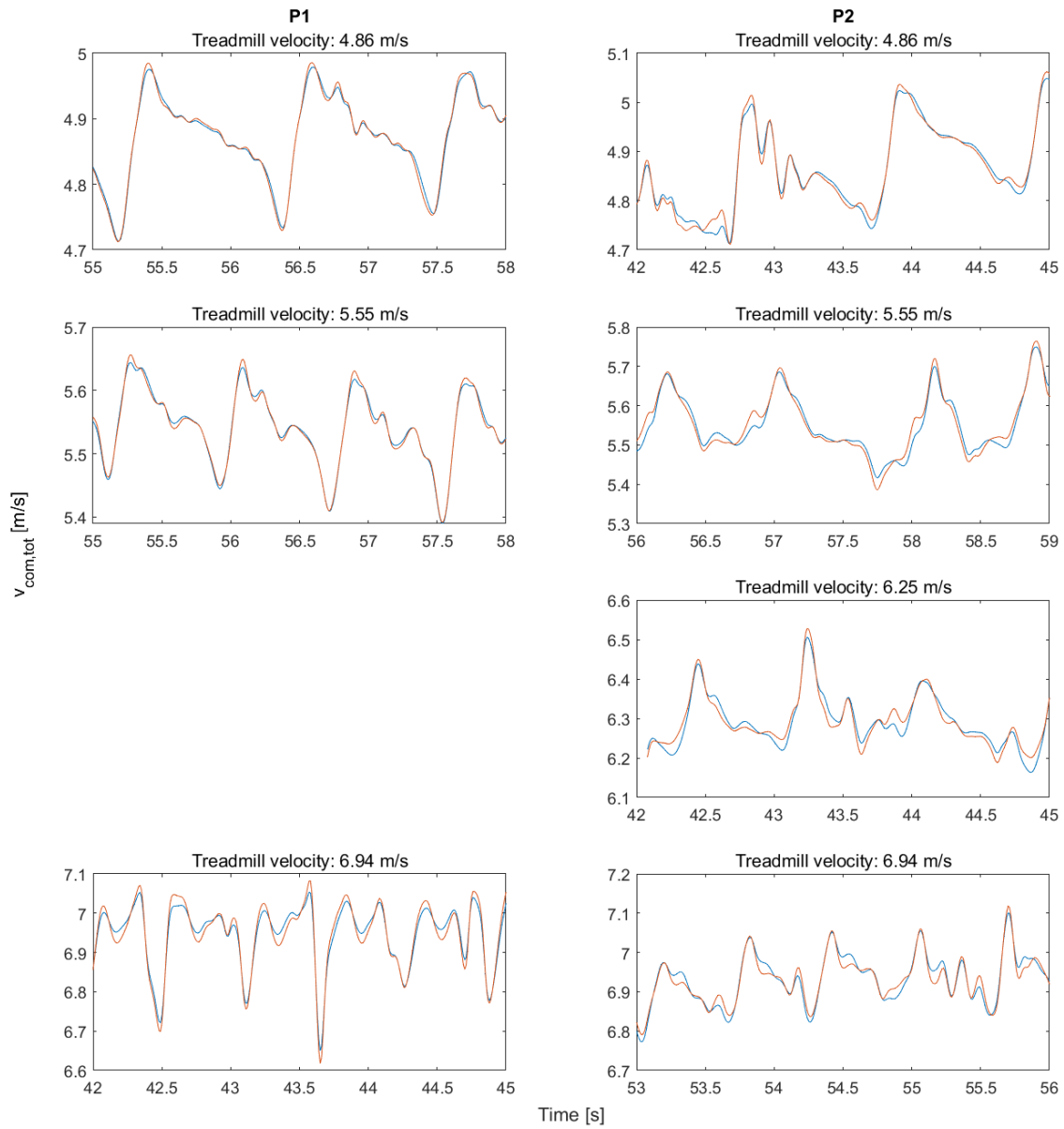
Figure C2. Velocity of the Centre of Mass using all upper body segments plotted over time. The blue line represents the $v_{com,tot}$ estimation using standard body mass distribution. The orange line represent the $v_{com,tot}$ estimation using increased mass of 50% for all upper body segments.